ENVIRONMENTAL RESEARCH
LETTERS

PURPOSE-LED PUBLISHING™ Part of the ENVIRONMENTAL RESEARCH SERIES

LETTER • OPEN ACCESS

Theoretical evaluation on CO_2 removal potential of enhanced weathering based on shrinking core model

To cite this article: Anqi Chen *et al* 2023 *Environ. Res. Lett.* **18** 124018

ENVIRONMENTAL RESEARCH
LETTERS

LETTER

Theoretical evaluation on CO_2 removal potential of enhanced weathering based on shrinking core model

Anqi Chen, Zhuo Chen and Bo-Lin Lin*

School of Physical Science and Technology, ShanghaiTech University, Shanghai 201210, People's Republic of China
* Author to whom any correspondence should be addressed.

E-mail: linbl@shanghaitech.edu.cn

Keywords: enhanced weathering, carbon dioxide removal, theoretical modeling

Supplementary material for this article is available online

OPEN ACCESS

RECEIVED
3 May 2023

REVISED
8 September 2023

ACCEPTED FOR PUBLICATION
31 October 2023

PUBLISHED
9 November 2023

Abstract

The discrepancy between current CO_2 emission trend and the targeted 1.5 °C warming requires the implementation of carbon dioxide removal (CDR) technologies. Among the engineered CDRs, enhanced weathering (EW) is expected to exhibit substantial potential for CO_2 removal, owing to the availability of abundant reserves of ultramafic rocks and demonstration of worldwide liming practice. While the shrinking core model (SCM) has been commonly adopted in previous theoretical and experimental studies, there still lacks a comprehensive assessment on the impacts of model parameters, such as rock particle size, size distribution, weathering rate and time length on the weathering kinetics and the resultant CDR potential. Herein, this study incorporates particle size distribution of rock powder into the surface reaction-controlled SCM, and conducts sensitivity analysis on EW's CDR potential quantitatively. Even fully powered by low-carbon energy in the optimistic case, the application of EW with olivine only achieves maximum CDR per unit of rock and energy consumption of 0.01 kg CO_2 per kg rock and 19 g per kWh at size of 8 and 22 μm respectively, indicating the limitations of EW. The derived optimal application parameters with olivine powers within 3.7–79 μm provide valuable insights into the practical real-world applications to achieve net CO_2 removal.

1. Introduction

Enhanced weathering (EW) is widely regarded as one of the candidate carbon dioxide removal (CDR) technologies with significant potential [1]. It involves spreading finely ground minerals in warm and humid environment to promote mineral weathering and CO_2 drawdown by reacting CO_2 with rock to form carbonate minerals ($CaCO_3$). In experimental and theoretical studies of CDR through EW, surface reaction-controlled shrinking core model (SCM) is often adopted to describe the kinetics of mineral weathering. The solid reactant continues shrinking down as the reaction with the surrounding fluid proceeds [2–6]. The derived mathematical model can be used to fit experimental data for kinetic parameters [4, 5] and to theoretically estimate the CDR potential of long-term and large-scale applications [3, 6].

In theoretical studies, extremely fine rock powders with a single uniform size was assumed to achieve a large weathering extent in a short period of time, *e.g.* diameter less than 30 μm for 100% of weathering [7–9]. However, this assumption is not in line with particle size distribution (PSD) of ground rock powders in real-world applications. Although some theoretical studies have attempted to incorporate PSD into their models, they typically rely on fixed distributions that neglect the impact of comminution methods and rock strength on the shape and range of the PSD [2, 3]. The impact of PSD of rock powders on the weathering extent and CO_2 removal potential has received limited attention in previous research. In reality, intensive grinding of rock powders leads to an increasing proportion of fine particles and creation of new surface area, which notably accelerates weathering rate (W_r) [10, 11]. However, a corresponding rise in grinding energy will cause additional CO_2 emissions that can counteract the CO_2 sequestration achieved via weathering [12]. The double-edged effect of rock sizes must be taken into consideration for the evaluation of the net CO_2 removal potential. Currently, there is still a lack of comprehensive

investigation into the impacts of model parameters, such as rock particle size, size distribution, weathering rate and weathering time length, on the weathering kinetics and the CO_2 removal potential when the overall emissions is taken into consideration as well.

Herein, this work introduced the PSD of rock powders into the surface reaction-controlled SCM and analyzed the impact of application parameters of EW on the weathering extent within a period of time. Sensitivity analysis on rock and energy types was also conducted regarding to energy consumption and CO_2 emissions during the application processes, *i.e.* mining, transportation, grinding, and spreading. Since the implementation of EW is energy and resource-intensive, figure of merits from the perspectives of energy and rock consumption was provided to gauge the real-world practical application.

2. Method

The dissolution of cations in minerals is affected by various factors, including the intrinsic physicochemical properties of minerals, solution chemistry, and environmental factors. In the field studies, sluggish dissolution kinetics on the mineral surface typically control the weathering process at ambient temperature and pressure [13, 14]. Therefore, surface-controlled SCM was adopted here to describe the overall weathering extent of rocks (φ) and carbonation process for CO_2 uptake. The relationship between the weathering extent of particles (X) with a certain size (D, unit: m) and time (t, unit: s) is expressed by:

$$X(W_r, t, D) = 1 - \left(\frac{D - 2V_m W_r t}{D}\right)^3 \quad (1)$$

where V_m denotes the molar volume of the minerals (unit: $m^3\ mol^{-1}$), W_r stands for the weathering rate (unit: $mol\ m^{-2}\ s^{-1}$). The full names and corresponding abbreviations of all parameters are listed in table 1.

The mathematical model further incorporated PSD of rock power represented by a bivariate function of Rosin–Rammler distribution, which is commonly used to fit the PSD of fine particles obtained from intensive grinding (see supplementary note 1 and 2) [15, 16]. For better understanding, the characteristic value of p80 size and the coefficient of variance (CV) were introduced as characteristic parameters of Rosin–Rammler distribution to provide granular information about the PSD statistically. The p80 size refers to the particle size at which 80% of the particles will pass when screened and the CV is the ratio of the standard deviation to the mean particle size. A large CV value indicates a high proportion of small particles in the distribution. Each set of p80 and CV values corresponds to a particular PSD.

It is assumed that the formation of pedogenic carbonates occurs within the soil, primarily relying on soil-retained water with limited capillary, percolating, and evaporating water. In the absence of a continuous water flushing into the soil, additional driving forces for percolating through aggregated particles, flushing off weathering-inhibiting surficial silica, and continuously removing carbonate and/or bicarbonates through soil drainage is mitigated. The precipitation of secondary carbonate is the major weathering product [17], which involves fixing one mole of CO_2 through the dissolution of each mole of magnesium or calcium ions from minerals expressed by equation (2). The maximum CO_2 removal potential of rocks (R_{CO2} in tons CO_2 per ton of rocks [18]) is therefore calculated to be 0.3 tons of CO_2 per ton of basalts (based on real-world basalt compositions [19]) and 0.63 tons of CO_2 per ton of pure forsterite (based on chemical formula Mg_2SiO_4) as the base and optimistic cases. The influence of temperature and hydrology on the weathering kinetics and CO_2 uptake is discussed in supplementary note 4 and 5

$$MgCaSi_2O_6 + 2CO_2 + 4H_2O \rightarrow MgCO_3 + CaCO_3 + 2H_4SiO_4. \quad (2)$$

The energy consumption for mining, transportation and spreading per unit mass of rock, denoted as E_i, was collected from literature [18] (table S1) while grinding energy was calculated using the proposed size-energy relationship (see supplementary note 3) [20]. Figure of merits, representing the CDR capability per unit of rock and energy consumption, was proposed as $M_{CO2,M}$ and $M_{CO2,E}$ (equations (3) and (4)) for sensitivity analysis of the influencing factors on CDR potentials, including rock types, energy intensity and carbon intensity of energy usage (EF_i) via use of fossil fuel (FF) and low carbon energy (LCE) as base and optimistic cases. Detailed parameters of sensitivity analysis are shown in table S1

$$M_{CO_2,M}(W_r, p80, R_{CO_2}, t) = \varphi \cdot R_{CO_2} - \Sigma E_i \cdot EF_i \quad (3)$$

$$M_{CO_2,E}(W_r, p80, R_{CO_2}, t) = \frac{\varphi \cdot R_{CO_2} - \Sigma E_i \cdot EF_i}{\Sigma E_i}. \quad (4)$$

3. Results and discussion

The impact of particle size on the CDR capability, regarding to both total energy consumption and CO_2 emissions, was initially investigated without considering the kinetic constraints of weathering, which means that the rock powders of all sizes undergo complete weathering, i.e. $\varphi = 100\%$ in equations (3) and (4). In this case, $M_{CO2,M}$ and $M_{CO2,E}$ represent the maximum net CDR capability that can be achieved for different rock types and energy usage scenarios at a specific particle size.

The curves of net CO_2 removal for two different rock components, from realistic basalt to idealized pure forsterite, are distributed in two distinct

Table 1. Abbreviations and their corresponding full forms.

Abbreviations	Full forms	Abbreviations	Full forms
CDR	Carbon dioxide removal	W_r	Weathering rate (mol m^{-2} s^{-1})
SCM	Shrinking core model	R_{CO2}	The maximum CO_2 removal potential of rocks (tons of CO_2 per ton of rocks)
PSD	Particle size distribution	φ	Weathering extent
CV	Coefficient of variance	E_i	Energy cost (kWh)
FF	Fossil fuel	EF_i	The carbon intensity of certain energy type (grams of CO_2 per kWh)
LCE	Low-carbon energy	$M_{CO2,M}$	CO_2 removal potential per unit mass of rocks (tons of CO_2 per ton of rocks)
p80	Particle size at which 80% of the particles will pass when screened (μm)	$M_{CO2,E}$	CO_2 removal potential per unit of energy (grams of CO_2 per kWh)
W	Work index (kWh/t)		

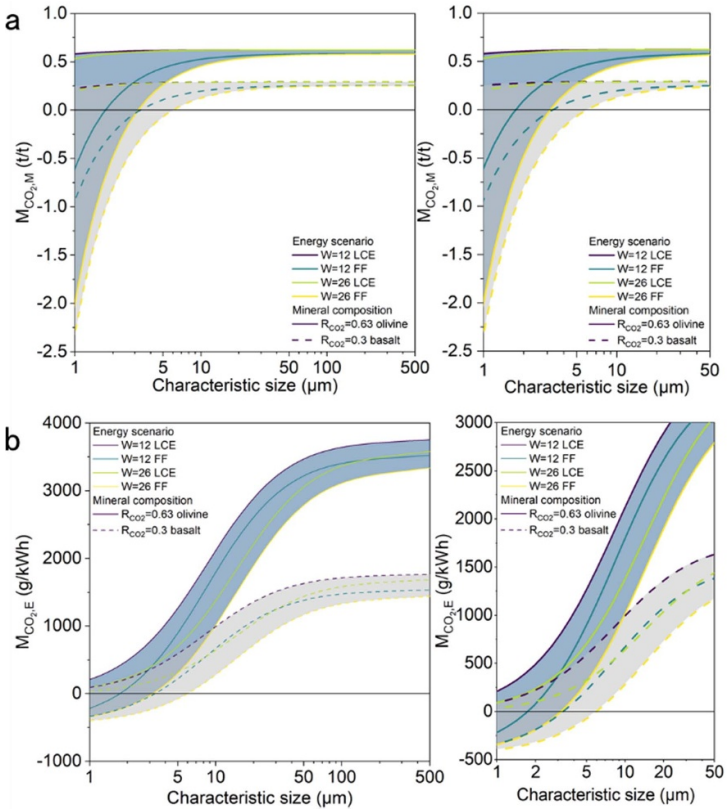

Figure 1. The relationship between CDR capability per unit of rock and energy consumption and rock size with complete weathering. (The *x*-axis is the characteristic size of p80 which represents the size distribution of rock powders. The right panel is partial enlargement of the left one. *W* represents work index (kWh/t) for the calculation of grinding energy. LCE and FF stand for low-carbon energy and fossil fuel energy, representing different energy scenarios. R_{CO2} represents the maximum CO_2 removal potential of rocks (tons of CO_2 per ton of rocks)).

areas marked as the blue and gray shaded areas representing $R_{CO2} = 0.3$ and 0.63 tons of CO_2 per ton of rocks, respectively (figure 1). Curves within each area depict different energy usage scenarios. With increasing particle sizes, the intrinsic CO_2 capture removal determined by rock components dominates the net CDR amount. However, as the characteristic particle size decreases, the increase in energy consumption and carbon emissions gradually reduces the net CDR amount per unit rock, moving away from the intrinsic values. Consequently, the influence of energy usage (energy consumption and carbon intensity of energy) becomes the dominates factor. The intersection of these curves with $M_{CO2,M} = 0$ and $M_{CO2,E} = 0$ corresponds to the lower bound of particle size to avoid net emissions. In the base case which is energy-intensive and dependent on FFs, even if the forsterite with the maximum intrinsic capability is applied and completely weathered, CO_2 emissions during EW application cannot be totally removed when the particle size

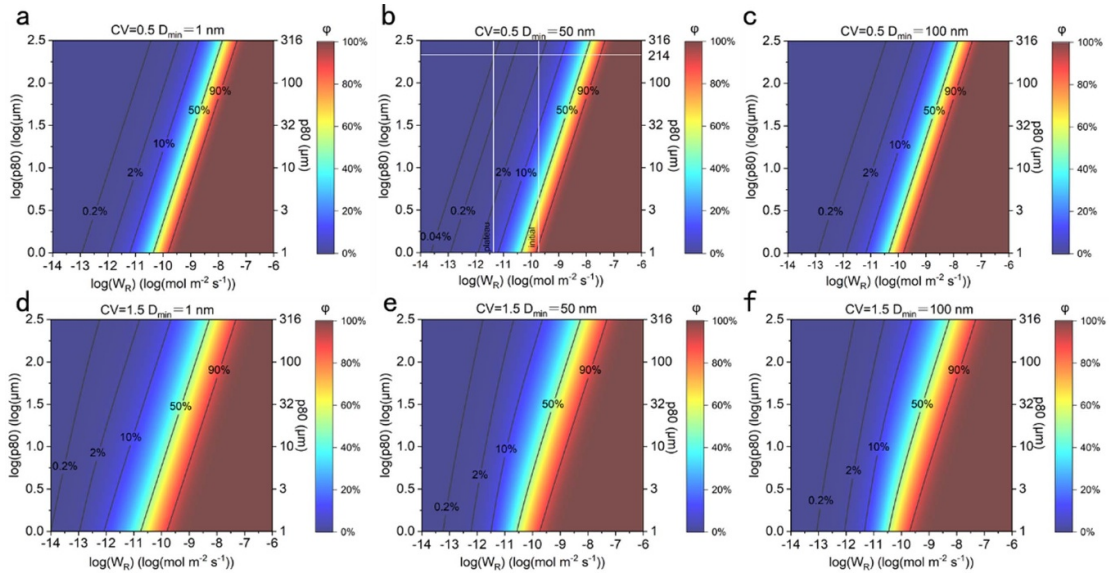

Figure 2. The relationship between particle size, weathering rate and weathering extent. (a)–(c) Theoretical modeling under CV = 0.5 and minimum size = 1, 50 and 100 nm, respectively. (d)–(f) Theoretical modeling under CV = 1.5 and minimum size = 1, 50 and 100 nm, respectively. Reference lines in c represent parameters recalculated from enhanced weathering experiment [4].

is less than 3 μm. By contrast, in the optimistic energy scenario, net CO_2 removal can be achieved with 100% weathering and any particle size.

In figure 1(a), two groups of curves with different R_{CO2} values overlap at particle sizes below 5 μm, whereas the overlap in figure 1(b) occurs at particle size below 10 μm. The intersection of the curves indicates that, for rocks with lower intrinsic CO_2 removal capabilities, optimizing energy usage through low-carbon energy and improving mechanical energy efficiency can lead to higher net CO_2 removal than olivine of the same size. Notably, it can be found that the overlap between the two rock-component areas in net unit-energy-cost CDR appears with relatively larger particle sizes (figure 1(b)) compared to the net unit-rock CDR curves (figure 1(a)), suggesting the impact on CO_2 offset due to particle size reduction is greater than that of energy consumption increment. Similarly, the size-dependent relative magnitude between the LCE-based curve with Bond work index (W) of 26 kWh/t and that based on FF with W of 12 kWh/t (figure 1(b)) is observed from their intersection points in the same rock component area (within the shaded area). As the particle size decreases, the change in the impact of particle size indicates a shift in the dominant factors affecting net CO_2 removal between CO_2 emissions offset and extra energy consumption. When particle size is greater than 10 μms which is more realistic in application, the nearly negligible influence of the CO_2 offset from auxiliary operations further emphasizes the significance of subsequent analysis on other influencing factors on net CDR potential.

In order to further incorporate the limitation of weathering kinetics into the evaluation of CDR potential, we extended our analysis to investigate the effects of particle size, size distribution, and weathering rate on rock weathering extent, considering the two boundary cases: basalts with R_{CO2} = 0.3 tons of CO_2 per ton of rocks in the base energy scenario, and ideal pure forsterite with R_{CO2} = 0.63 tons of CO_2 per ton of rocks in the optimistic energy scenario. Besides, the potential influence of parameter selection and underestimation of auxiliary energy cost in the theoretical model on the CDR potential was studies as well.

3.1. Impact of the selection of the minimum particle size in the mathematical model

In the mathematical model describing the surface-controlled shrinking core weathering kinetics, the minimum particle size of the rock powders in the PSD needs to be defined to calculate the weathering extent. The structure and properties of internal mineral crystals in rocks hinders the complete decomposition of all crystals into individual atoms even with highly intensive grinding in real-world mining practice [20]. Therefore, we selected 1 nm, 50 nm, and 100 nm as the minimum particle size for theoretical calculations to investigate the quantitative relationship between one-year weathering extent on particle size and W_r.

Figure 2 illustrates the weathering extent of the rock within one year under different weathering rates and PSD characterized by size p80 and CV. p80 is depicted as the vertical axis of the plots, and each horizontal line corresponds to a specific set of PSD and distribution features determined by p80 and CV values. CV of 0.5 indicates a relatively even distribution of large and small particles in the rock powders (figure 2(a)–(c)). When CV is equals to 0.5, the

selected minimum particle size of 1, 50, and 100 nm has almost no effect on the distribution of weathering extent contour lines. When CV is equal to 1.5, the peak of PSD shifts towards smaller particle sizes, and the proportion of fine particles in the rock powders increases. As the selected minimum particle size increases, the contour lines corresponding to the same weathering extent gradually shift to the right (figures 2(d)–(f)), revealing that a faster weathering rate is required. The shift is more prominent for contour lines of lower weathering extent. For instance, when the minimum selected particle size is 1, 50, and 100 nm with p80 of 10 μm, weathering extent of 0.2% requires a corresponding W_r of $10^{-13.4}$, $10^{-12.7}$, and $10^{-12.5}$ mol m^{-2} s^{-1}, respectively, while weathering extent of 10% requires corresponding W_r of $10^{-11.1}$, $10^{-10.9}$, and $10^{-10.8}$ mol m^{-2} s^{-1}, respectively. Thus, when fine particles dominate the size distribution, the selection of the minimum particle size greatly affects the theoretical calculation of weathering extent.

The trends observed above indicate that as the selected minimum particle size increases, the weathering extent of rock powders with the same PSD and W_r gradually decreases within one year. The reason is that the larger the minimum particle size is selected, the greater part of fine particles with size smaller than the minimum size are not included in the calculation, leading to a decrease in the overall weathering extent, which is particularly noticeable when the proportion of fine particles is high with CV of 1.5. According to the SCM, as the W_r slows down, the depth of the dissolution reaction on the particle surface decreases, and the weathering of fine particles contributes significantly to the overall weathering extent. This accounts for the observation that contours with smaller weathering extent ($\varphi = 0.02\%$) shift more to the right. Therefore, the minimum particle size should be determined based on the composition of rocks and type of grinding tools used in practice to avoid large deviations in the simulation of weathering extent.

Sarimai *et al* obtained forsterite powders with an average particle size of 345 nm after 40 h of ball milling. The grain size of the particles decreased from 53.8 nm to 18.78 nm after 5 h and obvious aggregation was observed [21]. In another similar study [22], 30 h of high-intensity ball milling gave forsterite powders with an average particle size of 147 nm and the proportion of particle size less than 50 nm was 25%. Besides, the reported grinding limit is in the range of 10–50 nm in the literature [20]. Subsequent theoretical analysis will be based on mathematical calculation with the minimum particle size of 50 nm. Although the selection of minimum particle size may cause deviation in the theoretical modeling as stated above, the influence is acceptable considering the uncertainty of reported weathering rates in the range of two to three orders of magnitude [23], which greatly exceeds the deviation caused by the selection of minimum particle size ($10^{0.1}$–$10^{0.7}$).

Laboratories studies with experimental setups mimicking the real world application of EW stills shows weathering extent with large discrepancy. An experimental study conducted with fast-weathering olivine in agitated seawater for 137 d showed an initial W_r of $10^{-9.72}$ mol m^{-2} s^{-1} with the PSD represented by p80 of 214 μm and CV of 0.5 approximately [4]. From the original data in the experiment, the one-year weathering extent was estimated to be about 2% through linear extrapolation of initial dissolution. In figure 2(b), the intersection point between the reference lines of initial W_r (the rate line labeled as 'initial') and the corresponding particle size gives a weathering extent of 1.8%, which is consistent with the experimental observation. However, this relatively fast W_r cannot be sustained, and a plateau was reached after *ca.* one month due to the accumulation of dissolved mineral cations, where the corresponding W_r and annual weathering extent is about $10^{-11.36}$ mol m^{-2} s^{-1} and 0.04%, respectively. In figure 2(b), the W_r reference line labeled as 'plateau' intersects with the particle size reference line at the point of approximately 0.045% of weathering in theoretical calculation, which agrees well with the experimental results as well. With the assumption of weathering with the retained water in soil, a W_r of $10^{-11.36}$ mol m^{-2} s^{-1} in the plateau region of the experiment due to local saturation can be used as a reference for following evaluation on CDR potential.

Apart from olivine modeled here, weathering extents of other minerals with specific weathering rate are in line with the modeling results here. For instance, in a 14 month soil-core experiments involving basalts [24], where particle sizes ranged from 125 to 250 μm, the observed weathering extent was derived to be approximately 0.04% within one year. In comparison, the yearly weathering rate of 0.32% for basalts was obtained in a 10 month experiment with similar setups but a water feeding rate 140 times higher [25]. Particle size with a p80 value of 74 μm was employed for basalts. The reported weathering rate for basalts in the former study (around $10^{-15.3}$ mol m^{-2} s^{-1}) was approximately two times slower than that in the latter one ($10^{-12.8}$–$10^{-13.4}$ mol m^{-2} s^{-1}) due to different weathering environments and particle size. The corresponding magnitude and range of weathering extent align with the trend in figure 2. Applying EW with weathering-accelerating factors, such as greater water feeding [26, 27], acidified soil due to organic and inorganic root exudates [28] and the reduction of particle size of minerals [29] can jointly contribute to greater weathering extent.

However, in two biotic and basalt-treated mesocosm studies with durations of 120 and 99 d, relatively higher yearly weathering extent of 17% and 7.4%

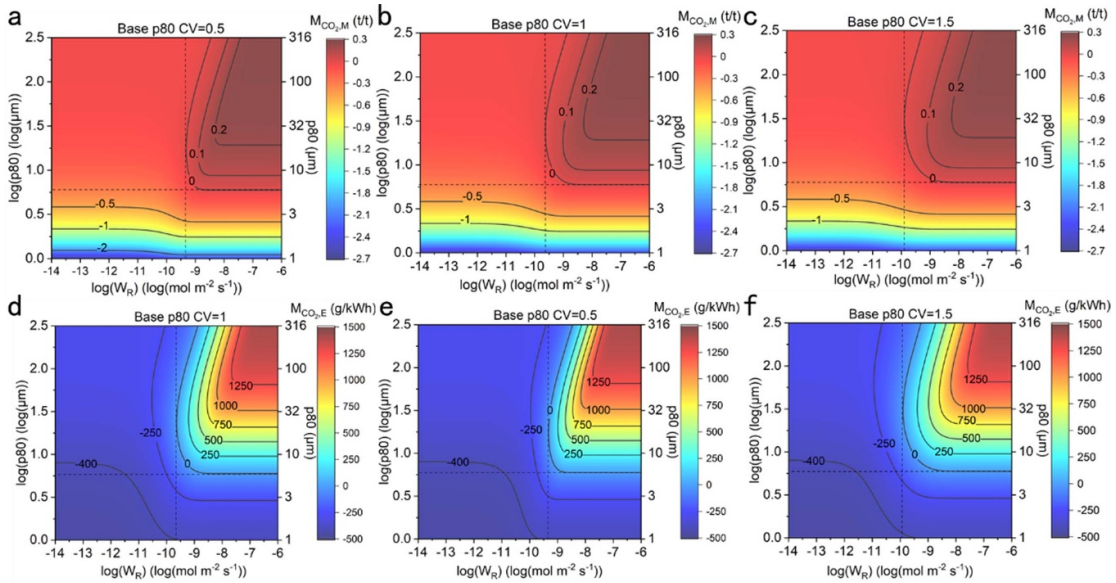

Figure 3. The relationship between particle size, weathering rate and on CO_2 removal potential for base cases. (a)–(c) CO_2 removal potential per unit mass of rock and (d)–(f) per unit of energy consumption with CV = 0.5, 1 and 1.5, respectively. (The grinding energy is calculated with p80).

were reported for basalts with p80 sizes of about 1250 and 250 μm, respectively [26, 27]. Notably, these two weathering extent were derived from the same 1D reactive transport model due to the relatively shorter experimental duration. It is essential to emphasize that the modeling results fall outside the scope of the discussion and comparisons in this study concerning only findings from field investigations.

3.2. Impact of the particle size, size distribution and weathering rate on CO_2 removal potential

In the previous section, the different trends for CV of 0.5 and 1.5 in figure 2 indicate the influence of PSD on the kinetics of weathering. Contour lines of rock weathering presented in figures 2(b) and (e) reveals that as the PSD of the rock powders narrows towards smaller particles, higher extent of one-year weathering is achieved under specific size and W_r. The resultant influence of PSD on CDR potential is further investigated in terms of per unit mass of rocks and unit energy consumption.

The impact of PSD, W_r, and energy usage scenario on the CDR potential shows different features within specific particle size and W_r ranges (figure 3). The horizontal and vertical black dashed lines are the tangents of the net zero CDR contour lines, representing the lower limits of particle size (particle size limit) and W_r (rate limit) required to achieve net CO_2 removal. Both the CO_2 offset from extra energy consumption and restriction of weathering extent determine that only rock powers with particle size and W_r larger than the corresponding limit have the potential for net CO_2 sequestration. With an increasing CV, the expansion of net sequestration area confined by particle size and rate limit implies that a higher proportion of small particles favors effective carbon sequestration in a wider range of particle sizes and weathering rates, which in turn increases the feasibility and flexibility of EW application.

However, even under the PSD with CV of 1.5 (figures 3(c) and (f)), net emissions are observed from the area on the left of the rate limit line where W_r is less than *ca.* 10^{-10} mol m^{-2} s^{-1} and below the particle size limit line where particle size is less than *ca.* 6 μm. When W_r is less than 10^{-10} mol m^{-2} s^{-1}, the weathering extent gradually increases as the rock particle size decreases. But with the limitation of W_r weathering extent of less than 10% can only be achieved over one year (figure 2). In comparison, when W_r is greater than 10^{-10} mol m^{-2} s^{-1}, an initial increase in the net carbon sequestration is followed by a sharp decline with decreasing particle size. This suggests that the significant increase in energy consumption and CO_2 emissions for size reduction further counteracts the carbon sequestration from weathering. The acceleration of weathering via size reduction is the main influencing factor in large size area, while the offset from CO_2 emissions of intensive grinding becomes dominant in the small size area. This phenomenon implies that rocks with W_r greater than 10^{-10} mol m^{-2} s^{-1} have an optimal particle size that achieves the maximum carbon sequestration under specific W_r.

According to the aforementioned W_r of olivine in weathering experiments ($10^{-11.36}$ mol m^{-2} s^{-1}), even under the condition of CV = 1.5 with a high proportion of small particle size, this rate fails to intersect with the contour line of net zero CO_2 removal, meaning net emissions under the constraint of W_r over one-year weathering (figures 3(c) and (f)). Net CO_2 removal can only be achieved within the range

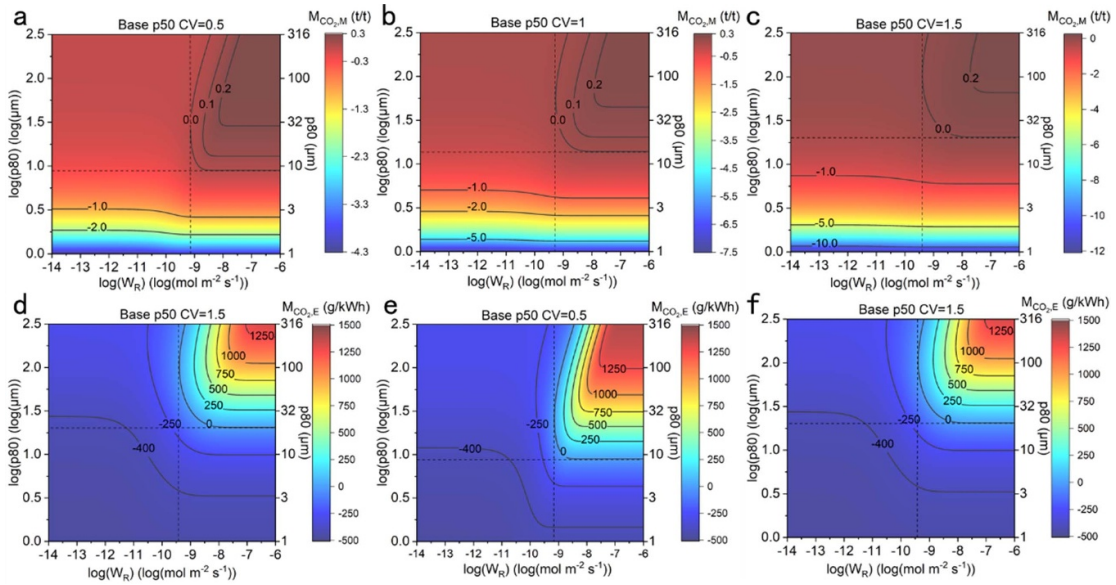

Figure 4. The relationship between particle size, weathering rate and on CO_2 removal potential for base cases. (a)–(c) CO_2 removal potential per unit mass of rock and (d)–(f) per unit of energy consumption with CV = 0.5, 1 and 1.5, respectively. (The grinding energy is calculated with p50).

of particle size and W_r limit lines. These results can be used as a valuable reference for the practical application of EW technology, including the selection of suitable rock types based on their weathering rate and the optimal target particle size for comminution.

3.3. Impact of underestimation of auxiliary energy cost on CO_2 removal potential

When CV is 1.5, the rock powders tend to have a relatively high proportion of fine particles. Taking the characteristic size of p80, which is typically used in the size-energy model [30], to calculate the grinding energy consumption can result in more than two-fold underestimation of energy consumption [31]. It arises particularly because p80 represents a relatively large size in the PSD and fail to account for the fine particles' size and proportion in the PSD. In order to investigate the potential underestimation of energy consumption, we calculated grinding energy using p50 as the characteristic size in the PSD defined by both CV and p80 for comparison. Since p50 is smaller than p80, the resultant grinding energy using p50 is higher, leading to a drop of CO_2 removal capability per unit-mass of rock and unit energy consumption (figures 4 and S1). As both p80 and p50 satisfy the PSD defined by CV and p80, the difference in CO_2 removal capability is solely determined by the energy scenario, which is independent of W_r (figures S1(a), (c) and (e)).

In the comparative analysis of the CO_2 removal capabilities calculated with p80 and p50 as the characteristic size for energy consumption (figure 4), it is evident that the particle size limit lines respond differently to the changes of CV. The former is not sensitive to the changes while in the latter one, particle size limit lines gradually shift towards larger particle sizes as CV increases. The increase of CV, requiring prolonged grinding time and an increase in grinding energy, will lead to a reduction in carbon sequestration under the same particle size and W_r. Consequently, the net carbon removal area slightly above the particle size limit in figures 4(a), (b), (d) and (e), will convert into net CO_2 emission with a CV of 1.5 (figures 4(c) and (f)). This trend is apparently rendered when calculated with p50. Meanwhile, the weathering rate limit lines in figures 3 and 4 demonstrate the same trend. When p50 is used to calculate grinding energy consumption and the PSD satisfies CV = 1.5 (figure 4(c)), net CO_2 removal can be achieved when the p80 of the PSD and the W_r is greater than 21 μm and $10^{-9.4}$ mol m^{-2} s^{-1} respectively.

The CO_2 removal capability per unit-mass of rock is significantly affected by the choice of characteristic size used for energy consumption calculations. Specifically, when p80 of the PSD is 1 μm and CV equates 0.5, 1, and 1.5, the difference in CO_2 removal capability per unit-mass of rock between the two approaches is 1.7, 4.9, and 9.5 tons of CO_2 per ton of rocks respectively. Moreover, the difference between the two approaches for CO_2 removal capability per unit energy consumption increases with the increase of CV values. These results indicate that using p50 as the characteristic size to calculate the grinding energy consumption is more suitable for cases where fine particles occupy a major proportion and require high-intensity grinding. Therefore, in the subsequent analysis of carbon sequestration potential, the calculation of grinding energy

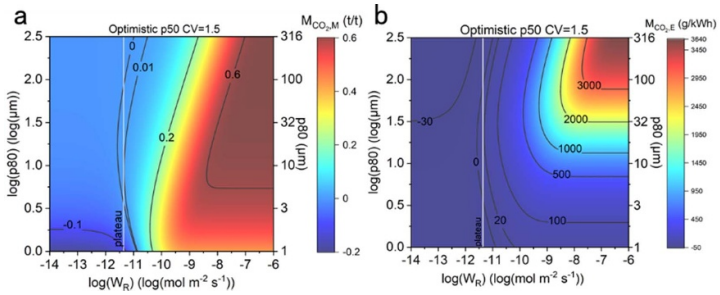

Figure 5. The relationship between particle size and weathering rate on CO_2 removal potential for optimistic cases. (a) CO_2 removal potential per unit mass of rock and (b) per unit of energy consumption with CV = 1.5 (the grinding energy is calculated with p50 and reference lines represent data from enhanced weathering experiment [4]).

consumption will rely on the use of p50 as the characteristic size.

3.4. Impact of energy usage scenario on CO_2 removal potential

To improve the CO_2 removal capability of the base case, it is necessary to optimize and enhance weathering from the perspectives of energy usage and rock types. The most favorable condition is represented by the optimistic case where low carbon intensity and reduced energy intensity are achieved.

In the optimistic case, the additional CO_2 emissions caused by grinding are greatly reduced, mitigating the offsetting effect on carbon sequestration and further expanding the effective range of net carbon removal under particle size and W_r. The intersection between the experimentally measured W_r of olivine and the net zero CO_2 removal contour line indicates that using olivine powders with p80 in the range of 3.7–79 μm can achieve net CO_2 removal. The maximum CO_2 removal capability per unit mass of olivine and per unit energy consumption is 0.01 tons of CO_2 per ton of rocks with p80 values of 8 μm and 19 g kWh^{-1} with p80 values of 22 μm, respectively (figure 5). To place these findings into context, Current and projected global total final energy consumption (TFC) of 418 EJ [32] and 616 EJ along current trajectory in 2050. Approximate 13% and 4% decline of annual global energy demand have come with profound sociopolitical and economic devastation in World War II [33] and the outbreak of Covid-19 pandemics [34], respectively. With such TFC scales and unaffordable energy cost, the net annual CDR potential in the optimistic scenario is estimated to be only 0.3 and 0.4 Gt at the 'world war cost' and 0.09 and 0.1 Gt at the 'against pandemic cost', respectively. This is far less than the approximately 12 Gt CO_2 emitted annually from hard-to-abate sectors [35]. To be competitive with another promising CDR technology direct air capture, whose CO_2 removal potential is derived as 505–805 g kWh^{-1} from life-cycle analysis [36, 37], weathering rate ranging from 10^{-10} to 10^{-8} mol m^{-2} s^{-1} is required for EW with suitable sizes.

Nonetheless, due to the inherent complexities associated with continuous monitoring and quantification, only a limited number of laboratory and field studies have delved deeper into the energy consumption and CO_2 offset from auxiliary operations. Consequently, apart from weathering extent, which can be readily derived from raw data, the annual and unit area of CO_2 removal capabilities reported in laboratory and field studies are overestimated, which makes it challenging to directly compare CO_2 removal capacity per unit-mass of rock and per unit of energy.

In a pot experiment, gross 0.013–0.18 t CO_2/t olivine was reported in the presence of perennial ryegrass and olivine powder with p50 size ranging from 2 and 50 μm during a 32 week growth and weathering period [38]. This corresponds to a range of 0.021–0.29 t CO_2/t olivine within a single year, extrapolated linearly. The variation in CO_2 removal potential per unit mass of rock arises from the different application rate of olivine powders. When considering the CO_2 offset from tertiary milling to ultrafine particles and taking the previously reported 174 g CO_2 emitted per kg of CO_2 sequestered into calculation, the lower boundary of the reported net removal potential aligns with our modeling results.

For comparison, notably smaller CO_2 removal potential, ranging from 0.105 to 0.223 kg CO_2/t dunite (containing approximately 90% olivine) was observed [29]. This difference may be attributed to the exclusion of secondary carbonates as weathering products. Given the complexities of isolating variables that impact the dissolution process in field studies [39, 40], future evaluations will require models that incorporate climatic, hydrological, and geochemical influencing factors and their interactions on weathering for more precise assessments.

It should be emphasized that to attain the maximum carbon removal potential in the optimistic scenario, low-carbon energy must be employed during the entire process of EW application. Currently, the global mining industry consumed approximately

4% of the global TFC, resulting in carbon emissions that account for around 10% of energy-related greenhouse gas emissions. Apart from the issue of high energy intensity, the release of nickel into soil and the possibility of silica dust may arise concerns regarding the potential impact on human health. Thus, it is imperative to put significant efforts into the development of ultra-EW technology and detailed environmental monitoring.

4. Conclusion

Based on the surface reaction-controlled shrinking core model, this study quantitatively investigated the impact of rock particle size, size distribution, and weathering rate on the weathering kinetics and CO_2 removal potentials of EW. (1) The optimal application parameters including particle size, size distribution and weathering rate that achieves the maximum carbon removal potential can be determined. (2) The selection of an appropriate characteristic size of rock powder for the calculation of grinding energy holds notable importance in mitigating the underestimation of energy consumption. The dominant factors influencing the figure of merits for energy and rock consumption were identified within specific ranges of application parameters, which can serve as a valuable reference for real-world implementation.

Even fully powered by low-carbon energy in the optimistic case, the application of EW with olivine only achieves maximum CDR per unit of rock and energy consumption of 0.01 tons of CO_2 per ton of rocks and 19 g kWh^{-1} at size of 8 and 22 μm respectively, indicating the limitations of EW. While there are still scientific and technical uncertainties to be addressed, it is necessary to achieve techno-economic breakthroughs to establish EW as alternative strategy for achieving substantial CDR and reversing the trend of global warming.

Data availability statement

All data that support the findings of this study are included within the article (and any supplementary files).

Acknowledgments

We would like to express our gratitude to the financial support from the Science and Technology Commission of Shanghai Municipality (No. 21DZ1206200).

Conflict of interest

The authors declare no conflict of interest.

References

[1] Pathak M *et al* 2022 Technical summary *Climate Change 2022: Mitigation of Climate Change. Contribution of Working Group III to the Sixth Assessment Report of the Intergovernmental Panel on Climate Change* (Cambridge University Press)
[2] Rinder T and von Hagke C 2021 The influence of particle size on the potential of enhanced basalt weathering for carbon dioxide removal—Insights from a regional assessment *J. Clean. Prod.* **315** 128178
[3] Beerling D J *et al* 2020 Potential for large-scale CO_2 removal via enhanced rock weathering with croplands *Nature* **583** 242–8
[4] Montserrat F, Renforth P, Hartmann J, Leermakers M, Knops P and Meysman F J R 2017 Olivine dissolution in seawater: implications for CO_2 sequestration through enhanced weathering in coastal environments *Environ. Sci. Technol.* **51** 3960–72
[5] Kowalczuk P B, Didyk-Mucha A, Pawlowska A, Sadowski Z and Drzymala J 2016 Application of the shrinking core model for dissolution of serpentinite in an acid solution. *E3S Web of Conf.* vol 8
[6] Kelemen P B, McQueen N, Wilcox J, Renforth P, Dipple G and Vankeuren A P 2020 Engineered carbon mineralization in ultramafic rocks for CO_2 removal from air: review and new insights *Chem. Geol.* **550** 119628
[7] Strefler J, Amann T, Bauer N, Kriegler E and Hartmann J 2018 Potential and costs of carbon dioxide removal by enhanced weathering of rocks *Environ. Res. Lett.* **13** 034010
[8] Moosdorf N, Renforth P and Hartmann J 2014 Carbon dioxide efficiency of terrestrial enhanced weathering *Environ. Sci. Technol.* **48** 4809–16
[9] Taylor L L, Quirk J, Thorley R M S, Kharecha P A, Hansen J, Ridgwell A, Lomas M R, Banwart S A and Beerling D J 2015 Enhanced weathering strategies for stabilizing climate and averting ocean acidification *Nat. Clim. Change* **6** 402–6
[10] Palandri J L and Kharaka Y K 2004 A compilation of rate parameters of water-mineral interaction kinetics for application to geochemical modeling (U.S. Geological Survey)
[11] Myers C, Sasagawa J and Nakagaki T 2022 Enhancing CO_2 mineralization rate and extent of iron and steel slag via grinding *ISIJ Int.* **62** 2446–53
[12] Hangx S J T and Spiers C J 2009 Coastal spreading of olivine to control atmospheric CO_2 concentrations: a critical analysis of viability *Int. J. Greenh. Gas Control* **3** 757–67
[13] Black J R, Carroll S A and Haese R R 2015 Rates of mineral dissolution under CO_2 storage conditions *Chem. Geol.* **399** 134–44
[14] Renforth P and Henderson G 2017 Assessing ocean alkalinity for carbon sequestration *Rev. Geophys.* **55** 636–74
[15] Wang Y and Forssberg E 2000 Product size distribution in stirred media mills *Miner. Eng.* **13** 459–65
[16] Petrakis E, Karmali V, Bartzas G and Komnitsas K 2019 Grinding kinetics of slag and effect of final particle size on the compressive strength of alkali activated materials *Minerals* **9** 714
[17] Knapp W J and Tipper E T 2022 The efficacy of enhancing carbonate weathering for carbon dioxide sequestration *Front. Clim.* **4** 928215
[18] Renforth P 2012 The potential of enhanced weathering in the UK *Int. J. Greenh. Gas Control* **10** 229–43
[19] Lewis A L *et al* 2021 Effects of mineralogy, chemistry and physical properties of basalts on carbon capture potential and plant-nutrient element release via enhanced weathering *Appl. Geochem.* **132** 105023
[20] Martins S 2020 Size-energy relationship exponents in comminution *Miner. Eng.* **149** 106259
[21] Sarimai S, Ratnawulan R, Ramli R and Fauzi A 2018 Effect of milling time on particle size of forsterite (Mg_2SiO_4) from

South Solok District *IOP Conf. Ser.: Mater. Sci. Eng.* **335** 012004
[22] Cheng L, Liu P, Chen X, Niu W, Yao G, Liu C, Zhao X, Liu Q and Zhang H 2012 Fabrication of nanopowders by high energy ball milling and low temperature sintering of Mg_2SiO_4 microwave dielectrics *J. Alloys Compd.* **513** 373–7
[23] White A F and Brantley S L 2003 The effect of time on the weathering of silicate minerals: why do weathering rates differ in the laboratory and field? *Chem. Geol.* **202** 479–506
[24] Buckingham F L, Henderson G M, Holdship P and Renforth P 2022 Soil core study indicates limited CO_2 removal by enhanced weathering in dry croplands in the UK *Appl. Geochem.* **147** 105482
[25] Amann T, Hartmann J, Hellmann R, Pedrosa E T and Malik A 2022 Enhanced weathering potentials—the role of in situ CO_2 and grain size distribution *Front. Clim.* **4** 929268
[26] Kelland M E *et al* 2020 Increased yield and CO_2 sequestration potential with the C_4 cereal Sorghum bicolor cultivated in basaltic rock dust-amended agricultural soil *Glob. Change Biol.* **26** 3658–76
[27] Vienne A, Poblador S, Portillo-Estrada M, Hartmann J, Ijiehon S, Wade P and Vicca S 2022 Enhanced weathering using basalt rock powder: carbon sequestration, co-benefits and risks in a mesocosm study with Solanum tuberosum *Front. Clim.* **4** 72
[28] Haque F, Santos R M, Dutta A, Thimmanagari M and Chiang Y W 2019 Co-benefits of wollastonite weathering in agriculture: CO_2 sequestration and promoted plant growth *ACS Omega* **4** 1425–33
[29] Amann T, Hartmann J, Struyf E, de Oliveira Garcia W, Fischer E K, Janssens I, Meire P and Schoelynck J 2020 Enhanced weathering and related element fluxes—a cropland mesocosm approach *Biogeosciences* **17** 103–19
[30] Nikolić V, García G G, Coello-Velázquez A L, Menéndez-Aguado J M, Trumić M and Trumić M S 2021 A review of alternative procedures to the bond ball mill standard grindability test *Metals* **11** 1114
[31] Martins S 2016 Size–energy relationship in comminution, incorporating scaling laws and heat *Int. J. Miner. Process.* **153** 29–43
[32] International Energy Agency (IEA) 2022 Key world energy statistics 2021 (International Energy Agency (IEA)) (available at: www.iea.org/reports/key-world-energy-statistics-2021)
[33] International Energy Agency (IEA) 2020 Global energy review 2020 (International Energy Agency (IEA)) (available at: www.iea.org/reports/global-energy-review-2020)
[34] Dale S 2021 BP statistical review of world energy (BP Plc) pp 14–16 (available at: www.bp.com/content/dam/bp/business-sites/en/global/corporate/pdfs/energy-economics/statistical-review/bp-stats-review-2021-full-report.pdf)
[35] Energy Transitions Commision 2018 Mission possible: reaching net-zero carbon emissions from harder-to-abate sectors (available at: www.energy-transitions.org/publications/mission-possible/)
[36] Deutz S and Bardow A 2021 Life-cycle assessment of an industrial direct air capture process based on temperature–vacuum swing adsorption *Nat. Energy* **6** 203–13
[37] Madhu K, Pauliuk S, Dhathri S and Creutzig F 2021 Understanding environmental trade-offs and resource demand of direct air capture technologies through comparative life-cycle assessment *Nat. Energy* **6** 1035–44
[38] Ten Berge H F M, van der Meer H G, Steenhuizen J W, Goedhart P W, Knops P and Verhagen J 2012 Olivine weathering in soil, and its effects on growth and nutrient uptake in Ryegrass (Lolium perenne L.): a pot experiment *PLoS One* **7** e42098
[39] Larkin C S *et al* 2022 Quantification of CO_2 removal in a large-scale enhanced weathering field trial on an oil palm plantation in Sabah, Malaysia *Front. Clim.* **4** 959229
[40] Taylor L L, Driscoll C T, Groffman P M, Rau G H, Blum J D and Beerling D J 2021 Increased carbon capture by a silicate-treated forested watershed affected by acid deposition *Biogeosciences* **18** 169–88